

On transient oscillations of plates in moving fluids[☆]

I. David Abrahams^{a,*}, Gerry R. Wickham^b

^a *Department of Mathematics, University of Manchester, Oxford Road, Manchester M13 9PL, UK*

^b *Department of Mathematical Sciences, Brunel University, Uxbridge, Middlesex UB8 3PH, UK*

Received 20 February 1999; accepted 14 January 2000

Abstract

In recent years, various groups of researchers have looked at the two-dimensional motions of an undamped infinite thin elastic plate lying under a uniformly moving incompressible inviscid fluid. The plate is driven, usually by a single frequency time-harmonic line-source switched on at a finite time. The system's behaviour is interesting as it can be shown to be absolutely unstable for flow velocities above a critical value, and below this the long-time solution is convectively unstable (downstream of the source) for a sufficiently low forcing frequency. These results do not appear particularly plausible from a physical point of view, and there is some question regarding the realisation of long-time steady behaviour, and so this article attempts to examine ways in which the model problem can be improved. In particular, the effects of introducing plate thickness and fluid compressibility to the model are studied. This is carried out by comparing the morphology of the original and modified solutions in the complex wavenumber space. It is found that, in the limit of small fluid-to-plate density ratio, the two problems exhibit qualitatively identical behaviour. However, the addition of structural damping is shown herein to lead to a very different solution – the initial boundary value problem is absolutely unstable at all flow velocities. Various other modifications to the original model, including finiteness of the plate, three-dimensional effects and nonlinearity, are discussed and their impact on the long-time response of the system is assessed. © 2001 Elsevier Science B.V. All rights reserved.

1. Introduction

The problem of the interaction of flexible or compliant surfaces with moving fluids has long been of interest to researchers in the field of fluid dynamics, structural vibrations and latterly in structural acoustics. The former have essentially been interested in the hydrodynamical stability properties of such flows where the surface compliance can accentuate or impede the onset of, or add new, fluid instabilities such as those of Tollmien–Schlichting type [1,2]. The classical route to investigate stability in this context has been to look at the growth or decay of small or not-so-small travelling wave disturbances to the basic state for a system of infinite extent. However, in this approach

[☆] This is perhaps the last article authored by Gerry Wickham to be published posthumously since his untimely death on Christmas eve, 1995. The number of his papers to have appeared since then is testament to Gerry's enthusiasm at collaborative research and his abundance of ideas. This work arose from our difficulties in reconciling the results offered in articles [Wave Motion 6 (1984) 547; Phil. Trans. R. Soc. Lond. A 335 (1991) 557] with real world notions, and was discussed with some interest at the EUROMECH 316 Colloquium in Manchester in 1994. Since then the first author has developed ideas further, to the point presented herein. Gerry was a great friend and brilliant collaborator, and his absence has been a real loss to the international theoretical mechanics community.

* Corresponding author. Tel.: +44-161-275-5901; fax: +44-161-275-5819.
E-mail address: i.d.abrahams@ma.man.ac.uk (I.D. Abrahams).

there are usually a priori assumptions made regarding the spatial or temporal nature of the instability — simple analysis of the dispersion relation between wavenumber, k , and angular frequency, ω , of a wave is insufficient to deduce the presence of convective or absolute instabilities in a given initial boundary value problem.

Workers concerned with the behaviour of the structure, or wall motion, in the presence of a flow have traditionally employed a different approach to that mentioned above (see e.g. [3–6]). Here the structure is taken to be of finite extent and so a modal expansion for surface deflections can be posed. This allows an unforced boundary value problem to be reduced to an algebraic system of equations which, by Galerkin's methods, is solvable for the eigenvalues and eigenvectors. The eigenvalues yield the flow speed, or other physical parameter values, for divergence, flutter, etc. instability of the surface. This provides information regarding the absolute instabilities of a physical problem, but, as above, does not actually reveal the long-time outcome from any initial boundary value problem with specified forcing.

The topic of structural acoustics, where the forced vibrations of a flexible body are intimately coupled to fluid motion, has grown rapidly in importance over the last 30 years or so. For example, it is now well-known that acoustic wave diffraction by an obstacle can be significantly altered by making the body flexible rather than rigid. Similarly, waves in or on solid boundaries, or the resonant frequencies of standing waves in such objects, are significantly affected by immersing the body in a fluid — often the radiation damping, caused by acoustic energy leaking to infinity, is the most significant agent for energy loss in such systems [7]. To most structural acousticians, what is required for a problem is the large-time or steady response to time-harmonic forcing (provided by excitation of the body (radiation problem) or by a wave incident in the fluid from infinity (the scattering problem)). To determine this, it is, in principle, necessary to solve an initial boundary value problem where the source is switched on at, say, time $t = 0$ and allowed to oscillate sinusoidally for a long time until all the transient behaviour has died out. However, for most problems of interest in the field it transpires that the time-dependent solution can be gleaned more simply by assuming the scattered or radiated field oscillates at the forcing frequency and then solving a time-independent boundary value program. Note that, for infinite or semi-infinite domains, Fourier transform (including Wiener–Hopf) methods are applicable for such boundary value problems. If there are singularities of the integrand on the inverse integration path (i.e. on the real line) then it can be shown that the *correct* long-time solution can be deduced by adding dissipation to the model (which shifts singularities off the real line) and then taking the limit as damping tends to zero. Unfortunately, this approach is not applicable when the fluid is moving, or in other models where infinite energy supplies can destabilise the solution. When the model may permit convective or temporal instabilities then a more detailed study of the initial value problem is warranted.

Although various authors have previously examined structural acoustics problems with moving fluids (including [5,8]), the first to address the question of absolute and convective instabilities in this context were Brazier-Smith and Scott [9]. (Note that for infinite domains and in the long-time limit, an absolute instability means exponential growth in time at any fixed spatial location, whereas a convective instability generates no amplification of a disturbance at such a point.) They wished to obtain the correct long-time behaviour of an infinite thin elastic plate, forced along one line on its surface, and immersed in a uniformly moving incompressible fluid. This was followed by a study by Crighton and Oswell [10] which offered a most detailed analysis of the long-time behaviour when the forcing oscillates sinusoidally after being switched on at $t = 0$. Both groups employed Fourier transforms in both space and time (with transform variables k and ω , respectively), and causality is ensured (zero solution for $t < 0$) by taking the Fourier inverse path in the complex frequency domain ω to lie above all singularities in this plane [11]. They then employed the method due to Briggs [12] of moving the ω integration contour down to the real line and at the same time, if necessary, deforming the Fourier inverse contour in the k -plane from the real line so that no singularities cross either integration path during this procedure. Sometimes the ω -contour cannot be brought down to the real line because singularities in the k -plane, originally on either side of the contour, move together thereby *pinching* the contour and so preventing deformation to avoid singularities touching or crossing the path. At this point the ω -contour cannot be lowered any further and hence it indicates the presence of a singularity in the upper half of the ω -plane. This yields an absolute, or temporal, instability at all spatial locations.

If deformation of the ω -contour to the real line can be accomplished, and the only singularities on the real line of the ω -plane are simple poles corresponding to the forcing frequency (i.e. all other singularities lie in the lower

half plane), then the long-time behaviour at a fixed spatial location is just that arising from this term [10]. That is, the response field oscillates at the forcing frequency. The contour in the k -plane is now uniquely determined in this procedure, and if it has been allowed to remain on the real line (perhaps indented about branch-points or poles lying on the real line) then no convective instabilities are found. Alternatively, if the k -contour has had to be deformed around singularities bounded away from the real-line then spatially growing waves must be included either upstream or downstream [11]. Brazier-Smith and Scott [9] and Crighton and Oswell [10] found, for the two-dimensional problem of an undamped infinite thin elastic plate submerged in a uniformly moving incompressible inviscid fluid, and excited by a line-source, that the problem is absolutely unstable for a nondimensionalised flow velocity of $U > U_c \approx 0.0742391$. Below this, and here we just give the briefest of details, the long-time solution is convectively stable for a nondimensionalised forcing frequency $\omega > \omega_p$, where $\omega_p \approx 0.00236463$ at $U = 0.05$. Between the frequencies $\omega_s < \omega < \omega_p$, where $\omega_s \approx 0.00225865$ at $U = 0.05$, there are neutral (i.e. real wavenumber) fluid loaded flexural waves on the plate, but when $\omega < \omega_s$ one of these waves gains an imaginary part to its wavenumber and so becomes convectively unstable downstream of the driver. Crighton and Oswell found that the neutral waves launched on the plate when $\omega_s < \omega < \omega_p$ are anomalous in that some of them are negative energy waves and have group velocity directed towards the driver. Not surprisingly, they also discovered that after a long time, the work done by the driver per cycle is negative for all forcing frequencies $\omega < \omega_p$.

This paper revisits the initial boundary value problem posed by Brazier-Smith and Scott and Crighton and Oswell. The reason for reappraising their results is due to the fact that they do not appear particularly plausible from a physical point of view. For example, for a glass pane in air at typical material values, the onset of absolute instability is predicted to occur at a very weak gust speed of just 0.04 m s^{-1} ! Clearly, this is regularly exceeded by wind flows past house windows without any apparent instability in their motion, and so some physical features not present in the Brazier-Smith and Scott model must be limiting the predicted growth. Another aspect of Crighton and Oswell's results which appears paradoxical is the negative work done by the driver and related convective instability, for frequencies below ω_p at speeds $U < U_c$. It is easily shown that if the forcing, switched on at time $t = 0$, oscillates with decaying amplitude in time, then this leads to a convective flexural wave instability with exponential growth *more severe* than in Crighton and Oswell's case or when the driver has increasing envelope in time!

A third and most important point worth reconsidering in Crighton and Oswell's analysis is the assumption that for large time and $U < U_c$ the field oscillates at the drive frequency. It can be demonstrated that sufficiently far upstream and downstream, i.e. x/t bounded away from 0 as $t \rightarrow \infty$, the argument employed by Crighton and Oswell to make this assumption are invalid. However much time has elapsed since the forcing commenced there is always an x value which is just experiencing the start-up disturbance travelling at a group velocity and frequency range not deducible from their results (see [10, Eq. 3.2]). As will be discussed later (see also [11]), this transient wave packet travelling downstream grows indefinitely with time and so cannot simply be ignored. The persistence of transient behaviour for a finite plate (panel) can also be anticipated to be important. The initial disturbance from the driver will reach the downstream edge of the plate, be propagated back upstream until it strikes the leading edge, and then propagates back downstream growing as it travels. It would therefore seem plausible that the finite length version of the Brazier-Smith and Scott model is, after long-time, absolutely unstable for all flow speeds and driver frequencies due to the multiple reflection of the convected transient disturbance. This has been found to be the case by Lucey [13] who performed a numerical investigation of the model at hand. We will offer further discussion of Lucey's results later in this article.

To address some of the reservations mentioned above for the Brazier-Smith and Scott model we wish to add various elements to the physical system to see if the solution is significantly modified. That is, are the Brazier-Smith and Scott [9] and Crighton and Oswell [10] long-time results *structurally stable* to various perturbations of the initial boundary value problem, or are they physically unrealisable solutions quite unrelated to solutions of models which are slightly different? We know that any physically realistic boundary value problem of the type discussed here will actually have a flexible plate of finite dimensions and nonnegligible thickness, and the fluid will be compressible and must move over the surface with some shear profile (in order to satisfy the no-slip condition). Both plate and fluid will be *lossy* and of course the governing equations of motion are nonlinear. Usually, in structural acoustics, a

good approximation to the physically realisable boundary value problem can be achieved by linearising the system (small amplitude approximation) and allowing the damping to be set to zero (for length and time scales on the order of the propagation wave number and speed). Similarly, infinite domains can be contemplated by applying a radiation condition at far distances. However, for reasons discussed above, it is not clear that such simplification can be made here. In this article (Section 5) we shall add the effects of plate thickness and fluid compressibility to the model. To see if these modify the original solution in a singular fashion it is sufficient to examine the morphology of both solutions in the complex wavenumber space. To compare results it is necessary to express the full time-dependent solution of Brazier-Smith and Scott and Crighton and Oswell's problems (impulse response in Sections 2 and 3, harmonic driver in Section 4) as Fourier inverse integrals in k -space only. The long-time behaviour can then be deduced by deformation of the integration contour into its steepest descent path — the morphology of the solution is essentially determined by the saddle and singularity locations in this k -plane. For brevity we do not show here the effects of fluid viscosity or a shear profile (instead of a uniform flow) on the long-time solution. In fact, they do not alter results in any qualitative fashion. However, Section 6 reveals that structural damping of the flexible surface does have a profound effect on the solution. A discussion is offered in the final section on the results presented herein, and other factors such as the role of plate nonlinearity. We also compare results with numerical calculations of Lucey [13] and offer suggestions for how finite plates could be tackled using the present approach.

2. The impulse response function

Consider an infinite elastic plate of mass per unit area m and bending stiffness B lying in the plane $y = 0$, where (x, y, z) is a Cartesian coordinate system. Suppose the region $y > 0$ is occupied by an incompressible inviscid fluid of density ρ_0 which is moving with uniform velocity $(U, 0, 0)$ and suppose the system is perturbed from this steady state by a unit line impulse acting on the plate at $x = 0$ in the positive y -direction. Taking the ensuing motion in the fluid–plate system to be sufficiently small, and purely two-dimensional because of the forcing and plate geometry, then the potential $\phi(x, y, t)$ of velocity fluctuations in the fluid are harmonic:

$$\frac{\partial^2 \phi}{\partial x^2} + \frac{\partial^2 \phi}{\partial y^2} = 0 \quad (2.1)$$

and the pressure in the fluid is given by the linearized Bernoulli equation

$$p(x, y, t) = -\rho_0 \left(\frac{\partial}{\partial t} + U \frac{\partial}{\partial x} \right) \phi(x, y, t), \quad (2.2)$$

where t is time. It will be assumed that the transverse displacement $\eta^*(x, t)$ of the elastic plate is governed by the Euler–Bernoulli thin plate equation

$$\left(m \frac{\partial^2}{\partial t^2} + B \frac{\partial^4}{\partial x^4} \right) \eta^*(x, t) = \delta(t) \delta(x) - p(x, 0, t), \quad (2.3)$$

where the first term on the right-hand side represents the applied line impulse at the origin. Also, the kinematic boundary condition at $y = 0$ is

$$\frac{\partial \phi}{\partial y}(x, 0, t) = \left(\frac{\partial}{\partial t} + U \frac{\partial}{\partial x} \right) \eta^*(x, t). \quad (2.4)$$

Finally we require the solution of Eqs. (2.1)–(2.4) subject to causality which is expressed as

$$\eta^*(x, t) \equiv 0, \quad \phi(x, y, t) \equiv 0, \quad t < 0. \quad (2.5)$$

Following Crighton and Oswell [10], we introduce dimensionless variables according to the scheme

$$\begin{aligned}
 x &\mapsto \frac{m}{\rho_0}x, & y &\mapsto \frac{m}{\rho_0}y, & t &\mapsto \frac{m^{5/2}}{\rho_0^2 B^{1/2}}t, & U &\mapsto \frac{\rho_0 B^{1/2}}{m^{3/2}}U, \\
 \phi &\mapsto \frac{B^{1/2}}{m^{1/2}}\phi, & \eta^* &\mapsto \frac{m}{\rho_0}\eta^*, & p &\mapsto \frac{\rho_0^3 B}{m^3}p, & \delta(x)\delta(t) &\mapsto \frac{\rho_0^3 B}{m^3}\delta(x)\delta(t),
 \end{aligned}
 \tag{2.6}$$

so that the solution may be expressed as a function of a single parameter, namely the dimensionless flow speed U . Thus, the pressure and plate relations for the dimensionless variables are just (2.2) and (2.3) with ρ_0 , m and B replaced by unity.

An explicit form for the motion of the plate is readily obtained by taking Fourier transforms with respect to x . Thus we define

$$\bar{\phi}(k, y, t) = \int_{-\infty}^{\infty} e^{-ikx} \phi(x, y, t) dx, \quad \bar{\eta}^*(k, t) = \int_{-\infty}^{\infty} e^{-ikx} \eta^*(x, t) dx,
 \tag{2.7}$$

etc. Eqs. (2.1) and (2.2) then give

$$\bar{\phi} = A(k, t) e^{-|k|y}, \quad \bar{p} = -e^{-|k|y} \left(\frac{d}{dt} + iUk \right) A(k, t),
 \tag{2.8}$$

where we have assumed without loss of generality that k may be taken to be real and that the disturbance decays with increasing depth y into the fluid; the undetermined function $A(k, t)$ must now be chosen to satisfy the remaining conditions at $y = 0$. The kinematic constraint (2.4) yields

$$A(k, t) = -\frac{1}{|k|} \left(\frac{d}{dt} + iUk \right) \bar{\eta}^*
 \tag{2.9}$$

and using this to eliminate $A(k, t)$ in the plate equation (2.3) we obtain

$$\frac{1 + |k|}{|k|} \frac{d^2 \bar{\eta}^*}{dt^2} + 2iU \frac{k}{|k|} \frac{d \bar{\eta}^*}{dt} + (k^4 - |k|U^2) \bar{\eta}^* = \delta(t).
 \tag{2.10}$$

A solution of this equation may be obtained by assuming that for each fixed k , $\bar{\eta}^*$ is continuous at $t = 0$. In this case, causality and the delta function forcing shows that we require a solution of the homogeneous equation corresponding to (2.10) which satisfies the initial conditions

$$\bar{\eta}^*(k, 0^+) = 0, \quad \frac{d \bar{\eta}^*}{dt}(k, 0^+) = \frac{|k|}{(1 + |k|)},
 \tag{2.11}$$

respectively. Thus we obtain

$$\bar{\eta}^*(k, t) = \frac{1}{|k|^{1/2} (|k|^3 + |k|^2 - U^2)^{1/2}} \sin \left[\frac{|k|^{3/2} (|k|^3 + |k|^2 - U^2)^{1/2} t}{1 + |k|} \right] \exp \left[-i \frac{kUt}{1 + |k|} \right].
 \tag{2.12}$$

Now taking inverse transforms we obtain

$$\eta^*(x, t) = \frac{1}{\pi} \int_0^{\infty} \frac{1}{k^{1/2} (k^3 + k^2 - U^2)^{1/2}} \sin \left[\frac{k^{3/2} (k^3 + k^2 - U^2)^{1/2} t}{1 + k} \right] \cos \left[kx - \frac{kUt}{1 + k} \right] dk.
 \tag{2.13}$$

For completeness we record the corresponding form for the velocity potential; expressions (2.8) and (2.9) give

$$\begin{aligned}
 \phi(x, y, t) &= \left(\frac{\partial}{\partial t} + U \frac{\partial}{\partial x} \right) \times \frac{-1}{\pi} \int_0^{\infty} \frac{e^{-ky}}{k^{3/2} (k^3 + k^2 - U^2)^{1/2}} \\
 &\quad \times \sin \left[\frac{k^{3/2} (k^3 + k^2 - U^2)^{1/2} t}{1 + k} \right] \cos \left[kx - \frac{kUt}{1 + k} \right] dk.
 \end{aligned}
 \tag{2.14}$$

In both (2.13) and (2.14) the integrand is analytic apart from a removable singularity at the origin and is absolutely integrable as $k \rightarrow \infty$. Thus, we conclude that for each fixed x and t the solution given by (2.14) exists. In the following section we shall consider the behaviour of η^* as $t \rightarrow \infty$.

3. Long-time behaviour of the impulse response

To study the asymptotic form of the solution for large times it is first convenient to rearrange (2.13) into a form suitable for the application of the method of steepest descent. Thus, it is easily verified that we may write

$$\eta^*(x, t) = \eta_+^*(x, t) + \eta_-^*(x, t), \quad (3.1)$$

where

$$\eta_{\pm}^*(x, t) = \pm \frac{1}{2\pi} \Re \int_0^{\infty} \frac{e^{i(kx - \omega_{\pm}(k, U)t)}}{\chi(k, U)} dk, \quad (3.2)$$

where

$$\chi(k, U) = k^{1/2}(U^2 - k^2 - k^3)^{1/2} \quad (3.3)$$

and

$$\omega_{\pm}(k, U) = \frac{k}{1+k}(U \pm i\chi(k, U)). \quad (3.4)$$

Unlike in (2.13), the integrands in (3.2) are not entire functions of k ; in particular we are obliged to make a consistent choice of the branch of χ in each term. This will be particularly important when we come to deform the contours of integration on to paths of descent. Firstly, note that the cubic factor $U^2 - k^2 - k^3$ has precisely one positive root k^* , say; the remaining two roots always have negative real part. With no loss of generality we shall arbitrarily cut the complex k -plane as shown in Fig. 1 and we shall take the Riemann surface for which χ is positive real for $0 < k < k^*$. It follows that the exponential phase function in the integral defining η_+^* grows exponentially in time for any fixed value of k within that interval, while the corresponding factor in η_-^* decays. In this section we shall concentrate on the motion $\eta^*(0, t)$ of the drive point as $t \rightarrow \infty$. We shall thus apply the method of steepest descents to the integrals in (3.2) with $x = 0$.

The possible paths of steepest descent at infinity are given by

$$\Re \left(\lim_{k \rightarrow \infty} \omega_{\pm} \right) = 0, \quad \Im \left(\lim_{k \rightarrow \infty} \omega_{\pm} \right) < 0 \quad (3.5)$$

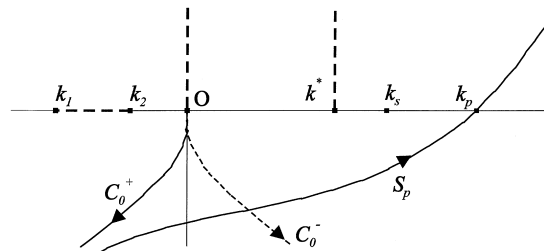


Fig. 1. The location of the branch-cuts of $\chi(k, U)$ (or $\omega_{\pm}(k, U)$) in the k -plane, the saddle-points k_s and k_p ($U < U_c$), and the steepest descent paths S_p , C_0^{\pm} for the integrals in (3.16).

and since

$$\chi(k, U) \rightarrow ik^2, \quad k \rightarrow \infty, \quad -\frac{3\pi}{2} < \arg(k) < \frac{\pi}{2}, \quad (3.6)$$

we see that the valleys for ω_{\pm} end along the rays $\arg(k) = \pm\pi/4, \pm3\pi/4$. Our strategy then is to seek deformations of the contours of integration from the origin through the saddle points in the right half plane ending along one or more of those paths of steepest descent.

The saddle points of the phase functions in (3.2) are where

$$\frac{\partial\omega_{\pm}}{\partial k}(k, U) = 0. \quad (3.7)$$

To determine the roots of these equations we note that

$$\frac{\partial\omega_{+}}{\partial k}(k, U) \frac{\partial\omega_{-}}{\partial k}(k, U) = \frac{P(k, U)}{4(1+k)^2(U^2 - k^2 - k^3)}, \quad (3.8)$$

where

$$P(k, U) = 16k^7 + 40k^6 + 25k^5 - 8U^2k^4 - 26U^2k^3 - 4U^2k^2 + U^4k + 4U^4, \quad (3.9)$$

so that there is a total of seven saddle points, shared between the two integrals. Using the principal of the argument, it can easily be shown that for every real value of U there are precisely two zeros of the numerator of $P(k, U)$ in the right half of the complex k -plane. Now either both these roots are real or they are complex conjugates. If they are real then they must satisfy

$$\frac{\partial\omega_{+}}{\partial k}(k, U) = 0, \quad (3.10)$$

since the chosen branch for χ excludes the alternative. Further, it is easily verified by inspection that, for U sufficiently small, ω_{+} does indeed have two real roots, one of $O(U)$ and one of $O(U^{2/3})$. Employing the notation of Crighton and Oswell [10], we denote the position of these roots by $k_s(U)$ and $k_p(U)$, respectively, and we find the asymptotic expansions

$$k_s = U + 4U^3 + 26U^4 + 252U^5 + 2484U^6 + 26050U^7 + 282618U^8 + O(U^9), \quad (3.11)$$

$$k_p = \left(\frac{2U}{5}\right)^{2/3} - \frac{9}{312500^{1/3}}U^{4/3} - \frac{216}{625}U^2 + O(U^{8/3}) \quad (3.12)$$

as $U \rightarrow 0$. It follows from the fact that they both also satisfy (3.10), that, as U increases to a certain critical value U_c , say, k_p and k_s coalesce at one of the solutions of the simultaneous equations

$$P(k, U) = 0, \quad \frac{\partial P(k, U)}{\partial k} = 0. \quad (3.13)$$

Remarkably, as was found by Crighton and Oswell [10], all the roots for (k, U) of this system may be found explicitly in closed form and it is easily verified that the relevant solution is

$$(k, U) = (k_c, U_c) = \left(2\sqrt{\frac{5}{3}} - \frac{5}{2}, \frac{5}{6} \left(\sqrt{244\sqrt{15} - 945}\right)\right) = (0.0819889, 0.0742391). \quad (3.14)$$

Beyond that critical value for U , k_p and k_s bifurcate into a complex conjugate pair. Again by inspection, it may be verified that the root of $P(k, U)$ with negative imaginary part always satisfies (3.10), while the root with positive imaginary part moves as U increases and may cross a branch-cut to become a solution of the other member of (3.7).

In summary, we conclude that, for $U < U_c$, there are two real saddle points in the right half plane at $k = k_p, k_s$ for the phase integral defining $\eta_+^*(0, t)$ and none in the corresponding domain for η_-^* .

When $U < U_c$, there are no critical points of the integrand defining $\eta_+^*(0, t)$ to the right of $k = k_p$. A local analysis shows that the path of steepest descent through that point intersects the real axis at an angle of $\pi/4$ and so it is easily verified that we may connect $k = k_p$ to the point at infinity along a continuous path of steepest descent S_p . Further, the contour of integration for $\eta_+^*(0, t)$, with $k > k_p$, may be deformed into that path, since (3.6) shows that the contribution from the arc at infinity vanishes. The continuation of S_p into the fourth quadrant does not return to the origin; indeed it may be shown by inspection that it descends into the valley in the third quadrant ending at infinity along the ray $\arg(k) = -3\pi/4$. We are thus faced with the task of connecting $k = 0$ to S_p to complete the required contour deformation. Near $k = 0$, we find

$$\omega_+(k, U) = U(k + ik^{3/2} + O(k^2)), \quad (3.15)$$

so that the path of steepest descent, C_0^+ , from the origin in the integrand defining $\eta_+^*(0, t)$ intersects the real axis at right-angles and turns into the third quadrant of the complex k -plane. Again by inspection, we are able to establish that C_0^+ descends into the valley $\arg(k) = -3\pi/4$ as $k \rightarrow \infty$. Similarly, the contour in the integral defining $\eta_-^*(0, t)$, may be deformed into C_0^- which starts at the origin at right-angles to the real axis and descends into the fourth quadrant along the valley $\arg(k) = -\pi/4$. We have drawn a schematic of the three contours S_p, C_0^\pm on the branch-cut location diagram, Fig. 1.

Having completed the deformation of the contours of integration onto global paths of steepest descent, we obtain three contributions to $\eta^*(0, t)$, namely,

$$\eta^*(0, t) = \frac{1}{2\pi} \Re \int_{C_0^+} \frac{e^{-i\omega_+(k, U)t}}{\chi(k, U)} dk + \frac{1}{2\pi} \Re \int_{C_0^-} \frac{e^{-i\omega_-(k, U)t}}{\chi(k, U)} dk + \frac{1}{2\pi} \Re \int_{S_p} \frac{e^{-i\omega_+(k, U)t}}{\chi(k, U)} dk. \quad (3.16)$$

For large t the values of the first two integrals are dominated by contributions from the origin in the complex k -plane and may be evaluated by Laplace's method [14, p. 121]. The remaining integral may be approximated using the ordinary method of steepest descent provided U is not close to U_c . Thus, we obtain finally

$$\eta^*(0, t) = \frac{1}{\sqrt{2\pi t U^3}} + 2\sqrt{\frac{U}{t\pi}} \Re \left[\frac{e^{-i(\omega_p t + \pi/4)}}{(k_p(\partial P/\partial k)(k_p, U))^{1/2}} \right] + o(t^{-1/2}), \quad 0 < U < U_c, \quad t \rightarrow \infty, \quad (3.17)$$

where $\omega_p = \omega_+(k_p, U)$. Note that we must take the argument of the denominator in the second term to satisfy

$$\left| \frac{\arg(k_p(\partial P/\partial k)(k_p, U))}{(\chi(k, U))^2} - \frac{3\pi}{2} \right| \leq \frac{\pi}{2}. \quad (3.18)$$

In particular, when $U < U_c$, we simply take the positive square root. This expression confirms the result of Brazier-Smith and Scott [9]: the deflection of the plate is bounded for all time, as can be seen from (3.17), as long as ω_p is real. However, when $U > U_c$, the frequency ω_p can be shown to have positive imaginary part and so η^* grows indefinitely in time for all x ; this is an absolute instability.

It has been necessary to go into some detail regarding the long-time asymptotics of this simple problem because we wish to investigate later the effects of changes to the boundary value problem. Once the morphology of the saddle and branch-cut structure is known, we can determine the effects of such modifications on the spatial and temporal behaviour of the model.

4. Response to continuous forcing

We now turn our attention to the case when the plate forcing is not an impulse, but is continuous, which was the focus of attention of Crighton and Oswell [10]. For simplicity we will be concerned with the case of simple

harmonic excitation, with (real) radian forcing frequency ω_0 , say (although it can prove interesting to complexify this frequency in order to analyse the system for growing or decaying forcings). The vibration is switched on at time $t = 0$ and we wish to determine the long-time behaviour of the system. This therefore, is the fundamental initial value problem for structural acoustics involving a moving fluid; only solutions which have a well defined steady-state solution as $t \rightarrow \infty$ are meaningful in this context, as will be discussed in subsequent sections.

The simple harmonic forcing may be written as

$$F(x, t) = \Re[e^{-i(\omega_0 t - \psi)} H(t)], \quad (4.1)$$

where $H(t)$ is the Heaviside step function, ω_0 is the angular forcing frequency, and ψ is an arbitrary constant phase shift. Thus, the right-hand side of the nondimensionalised form of the plate equation (2.3) is now

$$F(x, t) - p(x, 0, t) \quad (4.2)$$

and a solution to this initial boundary value problem can easily be obtained by convolving in time the impulse response η^* (2.13) with the new forcing (4.1). This yields

$$\eta(x, t) = \Re \left\{ e^{i(\psi - \omega_0 t)} \int_0^t e^{i\omega_0 t'} \eta^*(x, t') dt' \right\}, \quad (4.3)$$

which, as for η^* itself, exists for *any* fixed x and t . To compare the results of Crighton and Oswell [10] we must first interchange the t' and k (2.13) integrals and then perform an asymptotic analysis for large time. This interchange allows the t' integration to be accomplished, which yields after simplification

$$\begin{aligned} \eta(x, t) = \Re \left\{ \frac{ie^{i\psi}}{4\pi} \int_0^\infty \frac{e^{ikx}}{\chi(k, U)} \left(\frac{e^{-i\omega_+(k, U)t} - e^{-i\omega_0 t}}{\omega_+(k, U) - \omega_0} - \frac{e^{-i\omega_-(k, U)t} - e^{-i\omega_0 t}}{\omega_-(k, U) - \omega_0} \right) dk \right\} \\ + \Re \left\{ \frac{ie^{-i\psi}}{4\pi} \int_0^\infty \frac{e^{ikx}}{\chi(k, U)} \left(\frac{e^{-i\omega_+(k, U)t} - e^{i\omega_0 t}}{\omega_+(k, U) + \omega_0} - \frac{e^{-i\omega_-(k, U)t} - e^{i\omega_0 t}}{\omega_-(k, U) + \omega_0} \right) dk \right\}, \end{aligned} \quad (4.4)$$

where $\chi(k, U)$ and $\omega_\pm(k, U)$ are written in (3.3) and (3.4), respectively. Note that both integrands are entire, and so the integration paths may be deformed in any fashion. It should also be noted that if ω_0 is complex then ω_0 in the last integral should be replaced by its complex conjugate.

In order to perform the large t analysis, it is necessary to decompose both integrands in (4.4) into two parts, namely

$$\eta(x, t) = \Re \left\{ \frac{ie^{i\psi}}{4\pi} [I_1(x, t) - I_2(x, t)] \right\} + \Re \left\{ \frac{ie^{-i\psi}}{4\pi} [I_3(x, t) - I_4(x, t)] \right\}, \quad (4.5)$$

where

$$\begin{aligned} I_1(x, t) = I(x, t; \omega_+, \omega_0), \quad I_2(x, t) = I(x, t; \omega_-, \omega_0), \\ I_3(x, t) = I(x, t; \omega_+, -\omega_0), \quad I_4(x, t) = I(x, t; \omega_-, -\omega_0) \end{aligned} \quad (4.6)$$

$$I(x, t; \omega, \omega_0) = \int_0^\infty \frac{e^{ikx}}{\chi(k, U)} \frac{e^{-i\omega t} - e^{-i\omega_0 t}}{\omega - \omega_0} dk. \quad (4.7)$$

The integrands of I_1 – I_4 now contain branch points, and, if they are further decomposed into the two parts containing the separate exponents $e^{\pm i\omega_0 t}$ and $e^{-i\omega_\pm t}$, poles too in the complex k -plane. Thus, care must be taken when deforming the contours onto any new path. As mentioned in Section 3, a consistent choice of both the branch of χ and the position of the cuts is made as follows: χ is positive real for $0 < k < k^*$, and the cuts run from 0 to $i\infty$, k^* to $i\infty + k^*$, and k_1 to k_2 (see Fig. 1). With the k -plane cut as indicated it is a straightforward but tedious task to determine the

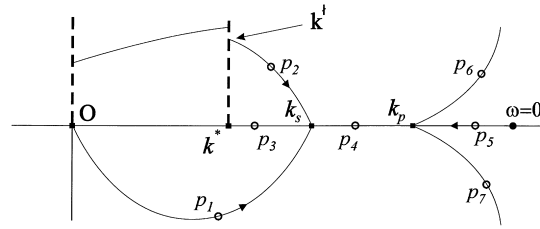


Fig. 2. Poles of $\omega_+(k, U) = \omega_0$ in the cut k -plane for $U < U_c$; p_1 exists for $0 < \omega_0 \leq \omega_s$, p_2 for $\omega^\dagger < \omega_0 \leq \omega_s$, where $\omega^\dagger = \lim_{\epsilon \rightarrow 0} \omega_+(k^\dagger + \epsilon, U)$, p_3 for $\omega_s < \omega_0 < \omega^*$ where $\omega^* = \omega_+(k^*, U)$, p_4 for $\omega_s < \omega_0 \leq \omega_p$, p_5 for $0 < \omega_0 \leq \omega_p$, and p_6, p_7 exist for $\omega_p < \omega_0$.

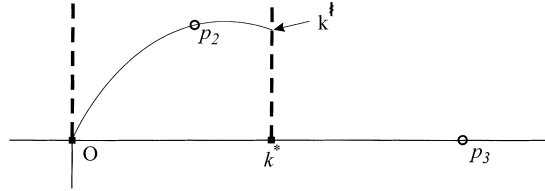


Fig. 3. Poles of $\omega_-(k, U) = \omega_0$ in the cut k -plane for $U < U_c$; p_2 exists for $0 < \omega_0 \leq \omega^\dagger$, $\omega^\dagger = \lim_{\epsilon \rightarrow 0} \omega_-(k^\dagger - \epsilon, U)$ and p_3 exists for $\omega^* \leq \omega_0$.

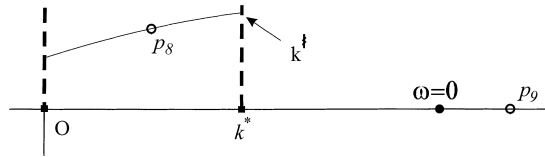


Fig. 4. Poles of $\omega_+(k, U) = -\omega_0$ in the cut k -plane for $U < U_c$; p_8 exists for $0 < \omega_0 \leq \omega^\ddagger$, $\omega^\ddagger = \lim_{\epsilon \rightarrow 0} \omega_+(k^\ddagger - \epsilon, U)$ and p_9 exists for $\omega_0 > 0$ (note p_9 is actually $-p_5$).

positions of the zeros of the denominators of the four integrals. For $U < U_c$, schematic diagrams are presented in Figs. 2–5 indicating the locus of these poles as ω_0 increases from zero. These figures also indicate the saddle points at k_s and k_p ((3.11) and (3.12)) occurring in I_1 and I_3 and the captions indicate the range of frequencies for which each indicated pole exists.

It should be noted that as ω_0 increases the poles can move from one Riemann surface to the other. For example, as ω_0 exceeds the value $\omega^\dagger = \lim_{\epsilon \rightarrow 0} \omega_-(k^\dagger - \epsilon, U)$ the pole p_2 in I_2 disappears, and becomes the pole p_2 in I_1 (hence the same labelling number). As Fig. 2 is quite complicated it is worth explaining the pole structure in a little detail. For low frequencies only three poles exist, namely p_1, p_2 and p_5 which move in the directions indicated as

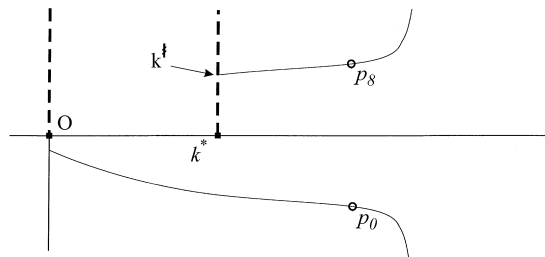


Fig. 5. Poles of $\omega_-(k, U) = -\omega_0$ in the cut k -plane for $U < U_c$; p_8 exists for $\omega^\ddagger < \omega_0$, $\omega^\ddagger = \lim_{\epsilon \rightarrow 0} \omega_-(k^\ddagger + \epsilon, U)$ and p_0 exists for $\omega_0 > 0$.

ω_0 increases. The pole p_2 appears at $\omega_0 = \omega^\dagger$, and this coalesces with p_1 at the point k_s when $\omega_0 = \omega_s$. As the frequency increases the two poles become real, indicated as p_3 and p_4 on Fig. 2, and p_3 moves onto the other sheet (Fig. 3) at $\omega_0 = \omega^* > \omega_s$ whereas p_4 coalesces with the pole p_5 at k_p when $\omega_0 = \omega_p$. For forcing frequencies exceeding ω_p , the only two poles of $\omega_+(k, U) = \omega_0 > \omega_p$ lie at p_6, p_7 as indicated.

To evaluate $\eta(x, t)$ for large t the procedure is as follows. Given the branch-cuts defined above, the four integral paths of I_1 – I_4 are deformed from along the positive real line to any location which avoids passing through the removable singularities in their integrands. Then each integral is decomposed into its two component parts, one with exponent $i(kx - \omega_\pm(k, U)t)$ and the other with $i(kx \pm \omega_0 t)$. Both terms now contain pole singularities in the integrands. The first of these integrals is deformed, for large t , into its steepest descent path discussed in the previous section (Fig. 1). Poles may be crossed during this deformation, which result in fluid-structural plate wave contributions. The latter integral has the simple exponent ikx in k and so its contour may be moved upwards (wrapping around the branch-cut at k^*) for $x > 0$, or downwards along the negative imaginary axis when $x < 0$. Again, any singularities crossed during deformation result in plate wave contributions to $\eta(x, t)$. As an example, I_1 yields, on deformation into its steepest descent paths, pole contributions from p_1, p_2 ($\omega_0 < \omega_s$) or p_3, p_4 or p_6 ($\omega_0 > \omega_p$) in $x > 0$ and p_5 ($\omega_0 < \omega_p$) or p_7 ($\omega_0 > \omega_p$) in $x < 0$. The descent integrals yield similar large time behaviour to that given in (3.17) plus the steady contribution. Note that the pole p_1 has negative imaginary part, and so for forcing frequency $\omega_0 < \omega_s$, there is a spatially unstable wave downstream of the drive point, confirming this result found by Crighton and Oswell [10] and Brazier-Smith and Scott [9]. Similarly, the anomalous waves p_3, p_4 , with neutral characteristics (real wavenumber) are found for higher frequencies, $\omega_s < \omega_0 < \omega_p$ whilst there are the usual attenuating terms in $x > 0$ (p_6), $x < 0$ (p_7) for $\omega_0 > \omega_p$.

Solving the initial value problem, rather than taking just the steady response (after completing the ‘pinch’ analysis [12]) is instructive as it clearly shows a unique solution to the boundary value problem with the growing terms for certain frequencies. Moreover, we know from the integral form for the solution $\eta(x, t)$ that it exists for all fixed values of x and t . Hence, for any large but finite times, and particularly for the case when there are spatially unstable plate terms, there will always be a sufficient distance $\pm x$ such that the transient terms become important and ultimately bound the growth — hence the steady results employed by Crighton and Oswell [10] will not recover the correct behaviour in these distant regions. Note that their solution is also invalid when $\omega = \omega_p$ because of the confluence of poles with the saddle point at k_p .

The following sections will examine the changes to the form of the solution presented here as modifications are made to the boundary value problem.

5. Thick plate and compressible flow formulation

The object of this section is to examine a *realistic* boundary value problem which does not have some of the shortcomings of the previous model. By this means it will be established if the stability results found in the previous sections are *structurally stable* to such perturbations of the model. In particular we wish to study the effects of changes in the boundary value problem on the morphology of the saddle-point/pole structure discussed in Section 4. The problem discussed in Section 2 may be criticised as too simplistic because (a) the structure is modelled by simple plate theory which yields a parabolic rather than hyperbolic equation, and (b) the fluid is incompressible and hence does not allow energy to dissipate through radiation damping. Both these points are now addressed.

Consider an infinite thick plate $0 \leq y \leq h$, $-\infty < x < \infty$ of homogeneous isotropic material which is wetted on $y = h$ by an inviscid compressible fluid filling the region $y > h$ and in uniform flow with speed U parallel to the plate. Let the Lamé moduli and density of the plate be (λ, μ) and ρ , respectively, so that the compressional and transverse wave speeds in the solid are

$$c_p = \sqrt{\frac{\lambda + 2\mu}{\rho}}, \quad c_t = \sqrt{\frac{\mu}{\rho}}. \quad (5.1)$$

The corresponding density and sound speed in the fluid will be denoted by ρ_0 and c . It follows that the velocity potential $\phi(x, y, t)$ and the Lamé displacement potentials $(\phi_s(x, y, t), \psi_s(x, y, t))$ satisfy the equations

$$\left(\nabla^2 - \frac{1}{c^2} \left(\frac{\partial}{\partial t} + U \frac{\partial}{\partial x} \right)^2 \right) \phi(x, y, t) = 0, \quad y \geq h, \quad (5.2)$$

$$\left(\nabla^2 - \frac{1}{c_p^2} \frac{\partial^2}{\partial t^2} \right) \phi_s(x, y, t) = 0, \quad \left(\nabla^2 - \frac{1}{c_t^2} \frac{\partial^2}{\partial t^2} \right) \psi_s(x, y, t) = 0, \quad 0 \leq y \leq h. \quad (5.3)$$

The elastic displacement vector and the fluid velocity are derived from

$$\mathbf{u}(x, y, t) = \text{grad } \phi_s(x, y, t) + \text{curl } \mathbf{e}_3 \psi_s(x, y, t), \quad (5.4)$$

$$\mathbf{v}(x, y, t) = \text{grad } \phi(x, y, t). \quad (5.5)$$

We assume that the system is excited by a time harmonic oscillatory line source of unit amplitude and frequency ω_0 which is switched on at time $t = 0$ at the point $(0, h)$ so that the boundary conditions may be expressed in the form

$$\frac{\partial}{\partial x} \left(\frac{\partial \phi_s}{\partial y} - \frac{\partial \psi_s}{\partial x} \right) + \frac{\partial}{\partial y} \left(\frac{\partial \phi_s}{\partial x} + \frac{\partial \psi_s}{\partial y} \right) = 0, \quad y = \begin{cases} 0, & -\infty < x < \infty, \\ h, & -\infty < x < \infty, \end{cases} \quad (5.6)$$

$$\lambda \nabla^2 \phi_s + 2\mu \frac{\partial}{\partial y} \left(\frac{\partial \phi_s}{\partial y} - \frac{\partial \psi_s}{\partial x} \right) = \rho_0 \left(\frac{\partial}{\partial t} + U \frac{\partial}{\partial x} \right) \phi + \delta(x) H(t) e^{-i\omega_0 t}, \quad y = h, \quad -\infty < x < \infty, \quad (5.7)$$

$$\lambda \nabla^2 \phi_s + 2\mu \frac{\partial}{\partial y} \left(\frac{\partial \phi_s}{\partial y} - \frac{\partial \psi_s}{\partial x} \right) = 0, \quad y = 0, \quad -\infty < x < \infty, \quad (5.8)$$

where $H(t)$ is the Heaviside function. The fluid–solid coupling problem is completed by imposing the kinematic constraint

$$\left(\frac{\partial}{\partial t} + U \frac{\partial}{\partial x} \right) \left(\frac{\partial \phi_s}{\partial y} - \frac{\partial \psi_s}{\partial x} \right) = \frac{\partial \phi}{\partial y}, \quad y = h, \quad -\infty < x < \infty. \quad (5.9)$$

Eq. (5.6) expresses the vanishing of the tangential stress on the plate surfaces while (5.7) states that the normal stress is continuous on the top surface, i.e. $\tau_{yy}(x, h, t)$ equals the fluid pressure there apart from at the point $(0, h)$ where the delta function accounts for the acoustic source. Finally, (5.9) equates the normal velocity of the plate with that of the fluid on the wetted side.

5.1. Nondimensionalised problem

We require a solution of Eqs. (5.2)–(5.9) subject to the causality requirement that the pressure and displacement fluctuations are zero for all time prior to $t = 0$. This initial boundary value problem may be nondimensionalised using the scalings defined in Section 2, together with

$$\phi_s \mapsto \frac{h^2}{\epsilon^2} \phi_s, \quad \psi_s \mapsto \frac{h^2}{\epsilon^2} \psi_s, \quad (5.10)$$

where $\epsilon = \rho_0/\rho$ is a dimensionless fluid loading parameter. Bearing in mind that, if ν is Poisson's ratio then

$$B = \frac{\mu h^3}{6(1-\nu)}, \quad m = \rho h \quad (5.11)$$

and it is easily verified that Eqs. (5.2)–(5.9) depend only on ϵ , ν and the ratio $\tau = c_p/c$ of sound speeds in the solid and fluid. Explicitly the partial differential equations become

$$\left(\nabla^2 - \epsilon^2 \tau^2 a^2 \left(\frac{\partial}{\partial t} + U \frac{\partial}{\partial x}\right)^2\right) \phi(x, y, t) = 0, \quad y \geq \epsilon, \quad (5.12)$$

$$\left(\nabla^2 - \epsilon^2 a^2 \frac{\partial^2}{\partial t^2}\right) \phi_s(x, y, t) = 0, \quad 0 \leq y \leq \epsilon, \quad (5.13)$$

$$\left(\nabla^2 - \epsilon^2 b^2 \frac{\partial^2}{\partial t^2}\right) \psi_s(x, y, t) = 0, \quad 0 \leq y \leq \epsilon, \quad (5.14)$$

in which

$$a^2 = \frac{(1-2\nu)}{12(1-\nu)^2}, \quad b^2 = \frac{1}{6(1-\nu)} \quad (5.15)$$

and the boundary conditions, for all $-\infty < x < \infty$, are

$$\frac{\partial}{\partial x} \left(\frac{\partial \phi_s}{\partial y} - \frac{\partial \psi_s}{\partial x}\right) + \frac{\partial}{\partial y} \left(\frac{\partial \phi_s}{\partial x} + \frac{\partial \psi_s}{\partial y}\right) = 0, \quad y = \begin{cases} 0, \\ \epsilon, \end{cases} \quad (5.16)$$

$$\frac{\nu}{1-2\nu} \nabla^2 \phi_s + \frac{\partial}{\partial y} \left(\frac{\partial \phi_s}{\partial y} - \frac{\partial \psi_s}{\partial x}\right) = \frac{\epsilon^3}{12(1-\nu)} \left(\frac{\partial}{\partial t} + U \frac{\partial}{\partial x}\right) \phi + \frac{\epsilon^3 \delta(x) H(t) e^{-i\omega_0 t}}{12(1-\nu)}, \quad y = \epsilon, \quad (5.17)$$

$$\frac{\nu}{1-2\nu} \nabla^2 \phi_s + \frac{\partial}{\partial y} \left(\frac{\partial \phi_s}{\partial y} - \frac{\partial \psi_s}{\partial x}\right) = 0, \quad y = 0 \quad (5.18)$$

with the kinematic constraint

$$\left(\frac{\partial}{\partial t} + U \frac{\partial}{\partial x}\right) \left(\frac{\partial \phi_s}{\partial y} - \frac{\partial \psi_s}{\partial x}\right) = \frac{\partial \phi}{\partial y}, \quad y = \epsilon, \quad -\infty < x < \infty. \quad (5.19)$$

5.2. Formal solution for the fluid velocity potential

By defining Fourier transforms (in both time and space) of the dependent variables appearing in the differential Eqs. (5.12)–(5.19), for example, in the following:

$$\phi_s(x, y, t) = \frac{1}{(2\pi)^2} \int_{-\infty}^{\infty} \int_{-\infty}^{\infty} \Phi_s(k, y, \omega) e^{i(kx - \omega t)} dk d\omega, \quad (5.20)$$

it is easily shown that the general solutions for Φ_s , Ψ_s , Φ are

$$\Phi_s(k, \omega) = A(k, \omega) \cosh \alpha(k, \omega) y + B(k, \omega) \sinh \alpha(k, \omega) y, \quad 0 \leq y \leq \epsilon, \quad (5.21)$$

$$\Psi_s(k, \omega) = C(k, \omega) \cosh \beta(k, \omega) y + D(k, \omega) \sinh \beta(k, \omega) y, \quad 0 \leq y \leq \epsilon, \quad (5.22)$$

$$\Phi(k, \omega) = E(k, \omega) e^{-\gamma(k, \omega)(y-\epsilon)}, \quad y \geq \epsilon, \quad (5.23)$$

where

$$\alpha(k, \omega) = (k^2 - \epsilon^2 a^2 \omega^2)^{1/2}, \quad \beta(k, \omega) = (k^2 - \epsilon^2 b^2 \omega^2)^{1/2}, \quad (5.24)$$

$$\gamma(k, \omega) = (k^2 - \epsilon^2 \tau^2 a^2 (\omega - kU)^2)^{1/2} \quad (5.25)$$

and a , b , given in (5.15), and $\tau = c_p/c$ are taken as $O(1)$ quantities. In order that (5.23) does not grow as $y \rightarrow \infty$ we choose $\Re(\gamma(k, \omega)) > 0$ in the whole complex k -plane for each value of ω . It is well known for the corresponding

case of a stationary fluid that this is sufficient to ensure that all acoustic disturbances are outgoing. Similarly for the elastic waves in the plate we impose the radiation condition by demanding that $\Re(\alpha(k, \omega)) > 0$ and $\Re(\beta(k, \omega)) > 0$. This leaves us with five unknown functions and five boundary conditions. Omitting, for brevity, the quite extensive algebraic manipulations, it transpires that the exact solution for $E(k, \omega)$ is

$$E(k, \omega) = \frac{\epsilon^5 b^4 \omega^2 (\omega - Uk) S_2(k, \omega)}{(\omega - \omega_0)(16k^2 \gamma(k, \omega) \beta(k, \omega) S(k, \omega) R(k, \omega) + \epsilon^5 b^4 \omega^2 S_2(k, \omega) (\omega - Uk)^2)}, \quad (5.26)$$

where

$$R(k, \omega) = m(k, \omega) \cosh \frac{\beta \epsilon}{2} \sinh \frac{\alpha \epsilon}{2} - \sinh \frac{\beta \epsilon}{2} \cosh \frac{\alpha \epsilon}{2}, \quad (5.27)$$

$$S(k, \omega) = m(k, \omega) \sinh \frac{\beta \epsilon}{2} \cosh \frac{\alpha \epsilon}{2} - \cosh \frac{\beta \epsilon}{2} \sinh \frac{\alpha \epsilon}{2}, \quad (5.28)$$

$$S_2(k, \omega) = m(k, \omega) \sinh \beta \epsilon \cosh \alpha \epsilon - \cosh \beta \epsilon \sinh \alpha \epsilon \quad (5.29)$$

and

$$m(k, \omega) = \frac{(2k^2 - \epsilon^2 b^2 \omega^2)^2}{4k^2 \alpha(k, \omega) \beta(k, \omega)}. \quad (5.30)$$

It is evident that the exact dispersion relation for the flow-loaded thick elastic plate is

$$16k^2 \gamma(k, \omega) \beta(k, \omega) S(k, \omega) R(k, \omega) + \epsilon^5 b^4 \omega^2 S_2(k, \omega) (\omega - Uk)^2 = 0. \quad (5.31)$$

The roots of this equation, say for a given real frequency ω , yield the spatial wavenumbers of all the possible propagating, leaky and evanescent modes in the fluid-plate system. It is interesting to note that, unlike the case of an in-vacuo plate, it is clear that the longitudinal and flexural modes are intrinsically coupled since (5.31) may not be factorised into the product of symmetric and antisymmetric parts. The form of $E(k, \omega)$ is very complicated and so the solution of (5.20) in general will require numerical investigation. However, it is interesting to compare the result here with that found in previous sections. To do this we will simply insist that the quantity $\epsilon = \rho_0/\rho$, i.e. the frequency independent fluid loading parameter, tends to zero whilst at the same time holding k, ω, a, b and τ fixed. Using an algebraic manipulation package it is a simple matter to show that

$$E(k, \omega) = \frac{(\omega - Uk)}{(\omega - \omega_0)((\omega - Uk)^2 + |k|(\omega^2 - k^4))} + O(\epsilon^2). \quad (5.32)$$

With this simple form for $E(k, \omega)$ employed in (5.23), and similar expressions for $A(k, \omega) - D(k, \omega)$, the ω integration in (5.20) can be performed explicitly. The result for $\phi(k, \omega)$, etc. can easily be compared with that given by (4.4) and they are found to be *identical*. Thus, this suitably scaled boundary value problem gives, in the limit of vanishing fluid-loading, the model of a forced Kirchhoff thin elastic plate under an incompressible fluid. What is rather surprising is that fact that these fairly unusual scalings, (2.6) and (5.10), allow the thin plate dispersion relation to arise very naturally out of the small fluid-loading asymptotics; this lends weight to the view held by the authors that approximate plate models are really only valid in fluid structural problems when the fluid is *light*.

The result given in (5.32) essentially confirms that the saddle-point structure discussed in Section 4, together with the consequent results regarding absolute instability, neutral and convectively unstable waves, etc. is *structurally stable* to the perturbation of the model discussed in this section. That is, by examination of the $O(\epsilon^2)$ correction term to the dispersion relation, it can easily be shown that the local morphology for the lightly loaded thick plate problem around the saddle-point ω_p, k_p is identical to that found previously. The saddles are shifted a small distance along the real line but the lines of $\Im(\omega_{\pm}) = 0$ remain as schematically indicated in Figs. 2–5.

6. Structural damping

In the preceding sections it was shown that the essential features of the complex k -plane outlined in Section 4, namely the branch-cuts, saddle-points and steepest descent paths, are not altered topologically by the addition of compressibility, or by an improvement/modification to the structural equation. Thus, the inherent deficiencies of fluid incompressibility or a parabolic wave equation, both of which admit infinite phase speeds, do not in themselves lead to the results discussed by Crighton and Oswell [10]. It can also be shown that *fluid viscosity does not affect the saddle-point structure nor the steepest descent path*. Thus, it seems that the initial boundary value problem is structurally stable to such changes to the governing and boundary equations, and hence the phenomenologically observed behaviour in this most primitive model is in some sense generic. However, we shall now show that this is not the case; in particular, the imposition of even the smallest amount of structural damping gives rise to a dramatic change in the solution.

We shall examine the effect of adding damping to the plate equation in two different ways. This is to demonstrate that the *precise* form of chosen damping is irrelevant, and that the arguments elucidated are in some sense generic. Firstly, we introduce viscoelastic effects in the stress–strain law, which, in the frequency domain, is modelled by including a small positive imaginary part in the bending stiffness B . Therefore, the dispersion relation arising in the first integral in (4.4) becomes

$$g(k, \omega, \mu) = (1+k)(\omega - \omega_+(k, U))(\omega - \omega_-(k, U)) = \omega^2(1+k) - 2\omega Uk + i\omega\mu k^5 - k^5 + U^2 k^2, \quad (6.1)$$

where $k > 0$ and μ is a small positive viscosity coefficient. Second, we suppose that the plate is backed by some absorbent material such as foam, which might effectively be modelled by a resistance proportional to the transverse plate velocity. Thus, the introduction of a linear term in $\partial\eta/\partial t$ in the plate equation yields

$$g(k, \omega, \mu) = \omega^2(1+k) - 2\omega Uk + i\omega\mu k - k^5 + U^2 k^2, \quad (6.2)$$

where again μ is a small dissipative factor. We wish to determine the change in the location of the dominant saddle point k_p , and to the corresponding value of ω_p for nonzero μ in both cases. Note that at (k_p, ω_p) we have

$$g(k_p, \omega_p, \mu) = 0, \quad \frac{\partial g}{\partial k}(k_p, \omega_p, \mu) = 0, \quad (6.3)$$

the latter condition arising from (3.7). Denoting the values of k_p, ω_p when $\mu = 0$ as k_0, ω_0 , respectively, then, for small μ , (6.1) may be expanded as

$$\begin{aligned} g(k_p, \omega_p, \mu) &= g(k_0, \omega_0, 0) + (k_p - k_0) \frac{\partial g}{\partial k}(k_0, \omega_0, 0) + (\omega_p - \omega_0) \frac{\partial g}{\partial \omega}(k_0, \omega_0, 0) \\ &\quad + \mu \frac{\partial g}{\partial \mu}(k_0, \omega_0, 0) + \mathcal{O}(\mu^2). \end{aligned} \quad (6.4)$$

Thus, to leading order, Eq. (6.3) evaluated at $\mu = 0$ gives

$$\omega_p = \omega_0 - \mu \frac{(\partial g / \partial \mu)(k_0, \omega_0, 0)}{(\partial g / \partial \omega)(k_0, \omega_0, 0)} + \mathcal{O}(\mu^2). \quad (6.5)$$

In the case of viscoelasticity this becomes

$$\omega_p = \omega_0 - \frac{i\omega_0 k_0^5 \mu}{2[\omega_0(1+k_0) - Uk_0]} + \mathcal{O}(\mu^2), \quad (6.6)$$

and for the absorbent backing

$$\omega_p = \omega_0 - \frac{i\omega_0 k_0 \mu}{2[\omega_0(1+k_0) - Uk_0]} + \mathcal{O}(\mu^2). \quad (6.7)$$

It is easily verified that

$$\omega_0(1 + k_0) - Uk_0 < 0, \quad (6.8)$$

for $U < U_c$, and so in both examples ω_p has a small positive imaginary part if μ is small and positive. It follows that the saddle point contribution to the impulse response (3.17) and the corresponding result for continuous forcing, grows like the following:

$$\frac{e^{\epsilon t}}{t^{1/2}}, \quad (6.9)$$

where ϵ is proportional to μ . Although ϵ may be small (6.9) can stay fairly constant over a long time before undergoing rapid growth.

Thus it would appear that the initial boundary value problem is *temporally unstable whatever the forcing or nondimensional flow velocity U* when we introduce small dissipative terms into the structural equation. In practice this would tend to suggest that the steady-state response predicted by the original ideal mechanical system is *not realisable!* However, for reasonably long observation periods, before the saddle point contribution dominates, the continuously forced system will exhibit two distinct radiated frequency components, one corresponding to the forcing frequency and the other at ω_p .

7. Concluding remarks

This article set-out to reformulate the solution of Brazier-Smith and Scott's [9] and Crighton and Oswell's [10] initial boundary value problem in a form explicit in time and as a Fourier integral over wavenumber. By this means the morphology of the saddle/pole structure was made apparent, and hence the long-time asymptotics could be obtained by contour deformation into steepest descent paths. The long-time asymptotics discussed in Section 4 were found to be consistent with those obtained by Crighton and Oswell for fixed x and $t \rightarrow \infty$ as long as $\omega \not\approx \omega_p$. However, it was revealed that as $t \rightarrow \infty$, x/t fixed, then the asymptotic results of Crighton and Oswell are invalid, and in fact the procedure in Section 4 must be modified to include the exponent ikx in the asymptotic phase factor. This alters the location of the saddle point, k_p , and omitting precise details for brevity, it can be shown that there is a window of positive x/t values (downstream) between which the saddle point ω_p has positive imaginary part (cf. Section 6). Thus, the start-up disturbance propagates downstream with ever-growing amplitude even in the absence of plate damping [11].

Sections 5 and 6 discussed morphological changes in the saddle/pole structure when the boundary value problem is modified to incorporate plate thickness and fluid compressibility, and plate damping, respectively. In the former case, light fluid loading yields the same structure of dispersion relation in the complex k -plane as for the thin plate model, and hence qualitatively identical behaviour. However, structural damping was shown to shift the saddle point, k_p , off the real line and hence destabilise the system (absolute instability) for all values of flow speed U .

The results presented here are perhaps a little unsatisfactory in that they do not directly answer in the affirmative the questions posed in Section 1. So, what mechanism, not incorporated here, removes or limits the predicted but physically unrealistic growth? Several candidates can be considered, namely finiteness of the plate, plate or fluid nonlinearity, or three-dimensional effects. In the last case, we could consider including this by a lateral restoring force in the plate. In fact, Peake [15] discussed such a model: axisymmetric disturbances on a circular cylindrical elastic shell immersed in a fluid which flows uniformly in the axial direction. He found, again, little qualitative difference between his results and those of Crighton and Oswell with regard to absolute instability, but quantitatively its onset occurs at much higher flow speeds when the nondimensionalised shell radius is of order unity. He also discovered critical radii values below which the anomalous and convectively unstable waves, respectively, were cut-off. However, Peake's results do not suggest that the aforementioned problems for the planar plate are resolved.

For an elastic panel of finite length in the flow direction, Lucey [13] has offered a comprehensive numerical study over a range of forcing frequencies. For the purposes of this article, his most important results are (a) the

long-time response has frequency components additional to that of the driver; (b) at early times the panel deflection is dominated by spatially growing waves (when driver frequency $\omega < \omega_p$) or absolute instability (when driver frequency $\omega > \omega_p$); (c) after long times the flexible panel shows disturbance amplitude growth at all locations for flows speeds above the critical divergence speed (see [3,5]) which is proportional to $(h/L)^{3/2}$ where h and L are the plate thickness and length respectively; this implies absolute instability at zero flow speed for infinite length plates, reinforcing the result of Section 6. Lucey suggests that finiteness of the panel can act as effective damping (via wave scattering at the edges, etc.) and his numerical discretisation inevitably introduce a damping effect, and so it is not too surprising that his model exhibits eventual temporal growth at all spatial points. However, here (Section 6) we predict eventual domination by the waves oscillating at the saddle frequency ω_p whereas Lucey can discern this frequency component at early times only. At longer times the temporal growth, at a higher rate than $\Im(\omega_p)$, dominates the response, and this is attributed to successive reflection of the convectively growing start-up wave packet. We note that the present analysis could be employed to discern the maximum growth rate and phase speed (i.e. the value of x/t) for this instability. It is worth mentioning that one possible way of tackling the finite panel problem by analytical means, in a fashion similar to that performed here, is to introduce an elastic plate with varying bending stiffness, $B(x)$. If $B(x) \rightarrow \infty$ as $x \rightarrow \pm\infty$ then the plate is effectively rigid at its ends, and so plate waves must reflect or lose their energy to the fluid as they propagate away from the origin. For particular choices of $B(x)$, Fourier transforms can still be applied, or else asymptotic approaches for slowly varying $B(x)$ are possible. This is currently under investigation by the first author.

Having discussed all the above modifications to the Crighton and Oswell model except one, attention must now be drawn to the role of nonlinearity in bounding the plate and fluid motions. The start-up transient wave packet grows indefinitely as it propagates downstream, and we have shown that damping always leads to absolute instability, so that the linear approximation must eventually become invalid. It therefore seems likely [7] that the dominant nonlinear term will be a membrane tension force due to the deflection of the plate from its planar states — this is a geometric nonlinearity. The tensional restoring force must eventually limit the plate amplitude, but quite how it does so is still under investigation. In conclusion, it is worth remarking that, unlike most other problems in the field of structural acoustics, this one appears to require the inclusion of both damping and nonlinearity to yield a *sensible* physical solution. That is, we suggest that the model is structurally unstable to perturbations in both damping and nonlinearity.

References

- [1] T.B. Benjamin, Effects of a flexible boundary on hydrodynamic stability, *J. Fluid Mech.* 9 (1960) 513–532.
- [2] A. Kornecki, Aeroelastic instabilities of infinitely long plates. I, *Solid Mech. Arch.* 3 (1978) 281–440.
- [3] C.H. Ellen, The stability of simply supported rectangular surfaces in uniform subsonic flow, *Trans. ASME E95* (1973) 68–72.
- [4] A.D. Garrad, P.W. Carpenter, A theoretical investigation of flow-induced instabilities in compliant coatings, *J. Sound Vibration* 84 (1982) 483–500.
- [5] I.D. Abrahams, Scattering of sound by an elastic plate with flow, *J. Sound Vibration* 89 (1983) 213–231.
- [6] A.D. Lucey, P.W. Carpenter, The hydroelastic stability of three-dimensional disturbances of a finite compliant panel, *J. Sound Vibration* 163 (1993) 527–552.
- [7] I.D. Abrahams, Acoustic scattering by a finite nonlinear elastic plate. I. Primary, secondary and combination resonances, *Proc. R. Soc. Lond. A* 414 (1987) 237–253.
- [8] I.D. Abrahams, G.A. Kriegsmann, E.L. Reiss, On the development and control of caustics in shear flows over elastic surfaces, *J. Acoust. Soc. Am.* 92 (1992) 428–434.
- [9] P.R. Brazier-Smith, J.F. Scott, Stability of fluid flow in the presence of a compliant surface, *Wave Motion* 6 (1984) 547–560.
- [10] D.G. Crighton, J.E. Oswell, Fluid loading with mean flow. I. Response of an elastic plate to localized excitation, *Phil. Trans. R. Soc. Lond. A* 335 (1991) 557–592.
- [11] P. Huerre, P.A. Monkewitz, Local and global instabilities in spatially developing flows, *Ann. Rev. Fluid Mech.* 22 (1990) 473–537.
- [12] R.J. Briggs, *Electron-stream Interaction with Plasmas*, MIT Press, Cambridge, MA, 1964.
- [13] A.D. Lucey, The excitation of waves on a flexible panel in a uniform flow, *Phil. Trans. R. Soc. Lond. A* 356 (1998) 2999–3039.
- [14] F.W.J. Olver, *Asymptotics and Special Functions*, Academic Press, New York, 1974.
- [15] N. Peake, On the behaviour of a fluid-loaded cylindrical shell with mean flow, *J. Fluid Mech.* 338 (1997) 387–410.